

Evaluation of PD-L1 Expression and Associated Tumor-Infiltrating Lymphocytes in Laryngeal Squamous Cell Carcinoma

Maria Vassilakopoulou¹, Margaritis Avgeris², Vamsidhar Velcheti¹, Vassiliki Kotoula^{3,4}, Theodore Rampias⁵, Kyriakos Chatzopoulos⁴, Christos Perisanidis⁶, Christos K. Kontos², Aris I. Giotakis⁷, Andreas Scorilas², David Rimm¹, Clarence Sasaki⁵, George Fountzilas⁴, and Amanda Psyrris⁸

Abstract

Purpose: Programmed death-ligand 1 (PD-L1; also known as CD274 or B7-H1) expression represents a mechanism of immune escape for cancer. Our purpose was to characterize tumor PD-L1 expression and associated T-cell infiltration in primary laryngeal squamous cell carcinomas (SCC).

Experimental Design: A well-annotated cohort of 260 operable primary laryngeal SCCs [formalin-fixed paraffin-embedded (FFPE) specimens] was morphologically characterized for stromal tumor-infiltrating lymphocytes (TIL), on hematoxylin/eosin-stained whole sections and for PD-L1 mRNA expression by qRT-PCR in FFPE specimens. For PD-L1 protein expression, automated quantitative protein analysis (AQUA) was applied on tissue microarrays consisting of two cores from these tumors. In addition, PD-L1 mRNA expression in fresh-frozen tumors and normal adjacent tissue specimens was assessed in a

second independent cohort of 89 patients with primary laryngeal SCC.

Results: PD-L1 mRNA levels were upregulated in tumors compared with surrounding normal tissue ($P = 0.009$). TILs density correlated with tumor PD-L1 AQUA levels ($P = 0.021$). Both high TILs density and high PD-L1 AQUA levels were significantly associated with superior disease-free survival (DFS; TILs: $P = 0.009$ and PD-L1: $P = 0.044$) and overall survival (OS; TILs: $P = 0.015$ and PD-L1: $P = 0.059$) of the patients and retained significance in multivariate analysis.

Conclusions: Increased TILs density and PD-L1 levels are associated with better outcome in laryngeal squamous cell cancer. Assessment of TILs and PD-L1 expression could be useful to predict response to immune checkpoint inhibitors. *Clin Cancer Res*; 22(3); 704–13. ©2015 AACR.

Introduction

The recent demonstration that blockade of PD-1/PD-L1 checkpoint pathway is effective for several cancers, including melano-

ma and non-small cell lung cancer, has led to the clinical testing of PD-1/PD-L1 inhibitors in head and neck squamous cell cancers (HNSCC). Immune checkpoints, such as PD-1, are manipulated by tumors to allow tumor growth that is unchecked by the immune system. Overexpression of programmed cell death-ligand 1 or 2 (PD-L1 or PD-L2) by tumor cells activates the PD-1/PD-L1 checkpoint pathway, by binding to PD-1 receptor, and attenuating the immune response. Antibodies targeting immune checkpoints, such as PD-1, binding to their ligands can "release the brakes" and induce immune response against the tumor.

Lyford-Pike and colleagues (1) showed that PD-1/PD-L1 interaction plays a role in HPV-associated oropharyngeal cancer by creating an "immune-privileged" site for initial viral infection and subsequent adaptive immune resistance once tumors are established supporting a rationale for therapeutic blockade of this pathway in patients with HPV-associated HNSCC. In addition, PD-1-expressing T cells were found to be a positive prognostic indicator in HPV-associated oropharyngeal carcinoma (2).

Two phase I studies have reported on safety and activity of PD1 checkpoint inhibitors in HNSCC. Fury and colleagues (3) tested the PD-L1 antibody MEDI4736 in patients with recurrent/metastatic (R/M) HNSCC. Six of 53 (11%) patients attained response as per RECIST to treatment and 17% demonstrated stable disease. Four of five responders evaluable for PD-L1 expression by IHC were PD-L1 positive. One of 23 HPV⁺ patients and 4 of 21 HPV-negative patients demonstrated RECIST response. Chow and

¹Department of Pathology, Yale University School of Medicine, New Haven, Connecticut. ²Department of Biochemistry and Molecular Biology, Faculty of Biology, University of Athens, Athens, Greece. ³Department of Pathology, Aristotle University of Thessaloniki School of Medicine, Thessaloniki, Greece. ⁴Laboratory of Molecular Oncology, Hellenic Foundation for Cancer Research, Thessaloniki, Greece. ⁵Department of Surgery (Otolaryngology), Yale University School of Medicine, New Haven, Connecticut. ⁶Department of Cranio-, Maxillofacial and Oral Surgery, Medical University of Vienna, Vienna, Austria. ⁷First Ear, Nose and Throat Clinics, Athens General Hospital "Hippokratation," University of Athens, Athens, Greece. ⁸Second Department of Internal Medicine, Section of Medical Oncology, "Attikon" University Hospital, University of Athens, Athens, Greece.

Note: Supplementary data for this article are available at Clinical Cancer Research Online (<http://clincancerres.aacrjournals.org/>).

M. Vassilakopoulou and M. Avgeris contributed equally to this article.

Current address for M. Vassilakopoulou: Centre Hospitalier Marc Jacquet, 2 Rue Fréteau de Penry, 77011 Melun, Seine et Marne and Hôpital Pitié-Salpêtrière, 47-83 Boulevard de l'Hôpital, 75013 Paris, France.

Corresponding Author: Amanda Psyrris, Second Department of Internal Medicine, Section of Medical Oncology, "Attikon" University Hospital, School of Medicine, University of Athens, 124 61 Athens, Greece. Phone: 30-210-583-1256; Fax: 30-210-583-1690; E-mail: dpsyrris@med.uoa.gr

doi: 10.1158/1078-0432.CCR-15-1543

©2015 American Association for Cancer Research.

Translational Relevance

Given the promising early clinical trial results of PD1 checkpoint inhibitors in patients with HNSCC, we used a well-annotated cohort of laryngeal cancer samples to characterize programmed death-ligand 1 (PD-L1) expression and T-cell content and the association with clinical outcome. We used qRT-PCR to assess *PD-L1* gene expression and a method of quantitative analysis to evaluate PD-L1 protein levels. A second well-annotated HNSCC cohort was also analyzed for *PD-L1* gene expression. TILs were measured by conventional IHC. Both high TILs and high PD-L1 automated quantitative protein analysis levels were significantly associated with superior DFS and OS. This is the first report of the prognostic importance of PD-L1 protein in HNSCC using a validated antibody. Biomarker studies in patients treated with PD1 checkpoint inhibitors should include assays combining PD-L1 expression and TIL characterization to assess whether the combination is more predictive of response to therapy than PD-L1 alone.

colleagues (4) evaluated MK3475, a PD1-targeting antibody, in PD-L1⁺ R/M HNSCC patients. The overall response rate (ORR) per RECIST version 1.1 by investigator assessment was 19.6% (95% confidence intervals; CI, 10.2%–32.4%). The median progression-free survival was 17.2 and 8.1 weeks for HPV⁺ and HPV-negative patients, respectively. These results support further development of PD1 checkpoint inhibitors in HNSCC. The superior results of the study by Chow and colleagues might be attributed to the fact that accrual was restricted to PD-L1 expressors. Preliminary studies in other tumors also suggest that clinical responses to immune checkpoint inhibitors are associated with increased levels of immune inhibitory signals, such as PD-L1, and with increased TILs or TIL subtypes (5–8).

The prognostic role of PD-L1 expression in tobacco-induced HNSCC has not been previously determined. Tobacco-induced HNSCC bear a large number of mutations that render them immunogenic.

Given the promising results of PD-1/PD-L1 inhibitors in clinical trials for R/M HNSCC, we used a well-annotated cohort of 260 laryngeal cancers (9) to characterize PD-L1 protein expression and TIL level in association with clinical outcome. We also evaluated PD-L1 mRNA levels in the abovementioned formalin-fixed paraffin-embedded (FFPE) cohort as well as in a second independent well-annotated cohort of 89 fresh-frozen specimens of paired tumors and normal adjacent tissues.

Materials and Methods

Patient cohorts

The study was conducted retrospectively in a cohort of 260 patients (cohort I) with primary SCC of the larynx (Table 1) treated with potentially curative resection, with or without external beam irradiation, between May 1985 and June 2008 at the Ear Nose and Throat Department of the Aristotle University of Thessaloniki (Thessaloniki, Greece). This cohort was used for histologic and PD-L1 assessments. A second independent well-annotated cohort of 89 fresh-frozen matched normal and primary laryngeal SCC specimens (cohort II) was used for the assessment

of PD-L1 mRNA levels (Fig. 1A). The patients of the second cohort were also treated with potentially curative resection, with or without external beam irradiation, at the First Ear, Nose and Throat Clinic (Athens General Hospital 'Hippokraton') of the University of Athens (Athens, Greece). A waiver of consent for the use of biologic material was provided by the Bioethics Committee for all patients included in the study before 2003. All patients included in the study after 2003 provided informed written consent for the provision of biologic material for future research studies. The study complied with the REMARK recommendations for tumor marker prognostic studies using biologic material (10).

Patients were endoscopically evaluated at regular monthly visits for the first year after surgery and every 2 months thereafter and staged with CT of the neck and chest every 6 months for the first 2 years after surgery and yearly thereafter or sooner if clinically indicated. Other diagnostic or staging procedures were performed upon clinical indications or symptom alert.

Histologic evaluation of tumor-infiltrating lymphocytes

Evaluation of tumor-infiltrating lymphocytes (TIL) was performed in hematoxylin-eosin (H&E)-stained whole FFPE sections, which were examined at X100 and X400 magnification fields using a conventional light microscope by a certified pathologist (K. Chatzopoulos) to ensure homogeneous assessment. Currently, different methods have been practiced for assessing tumor immune response with respect to lymphocytic infiltrations on FFPE sections, including morphologic evaluation of TILs (11–13), immunophenotyping (14, 15), and immunoscore with CD3/CD8 (16). Herein, we preferred to apply only the morphologic assessment as a first pragmatic and cost-effective approach of TILs evaluation in laryngeal cancer, since, to our knowledge, TILs have not yet been investigated in this setting. TILs density was calculated as a continuous variable by estimating the ratio of the area occupied by mononuclear cell infiltrates to the entire stromal area (% TILs = area occupied by mononuclear cells in tumor stroma/total stromal area; ref. 13). On the basis of the same recommendations, intratumoral lymphocytes, that is, those in immediate proximity to neoplastic cells within tumor nests, should be avoided. However, due to variations in tumor patterns of growth, such single lymphocytes occurring in small numbers were occasionally indistinguishable from stromal ones; nevertheless, these were scarce and not expected to have interfered with the overall TILs density. Sections from all available blocks (>1 block available in 53 cases) from the same tumor were evaluated and the average density was calculated, in order to adjust for TILs heterogeneity in each tumor.

Tissue microarray construction

H&E-stained slides from tissue blocks had been reviewed for adequacy of tumor tissue and estimation of the percentage of tumor cells in each case (9). Two hundred and sixty FFPE tissue blocks (cohort I) were histologically evaluated for tumor type, marked for tissue microarray (TMA) construction and, where necessary, for manual macrodissection. Low-density TMAs (~30 tumors per TMA block) were constructed with two tissue cylinders of 1.5 mm in diameter per tumor. The latter was performed on 8 μm unstained deparaffinized sections in order to increase tumor cell content in the subsequently extracted molecular templates, which contained >50% tumor cells in 64.2% of the cases and 30% to 50% in the remaining ones. The

Table 1. Clinicopathological features of the cohort I (N = 260) and cohort II (N = 89) of laryngeal SCC patients

| Cohort I (N = 260) | |
|-------------------------|----------------------------|
| Age | |
| Median (range) | 63 (36–82) |
| Variable | No. of patients N = 260 |
| Gender | |
| Male | 249 (95.8%) |
| Female | 11 (4.2%) |
| Tumor (T) stage | |
| T1 | 17 (6.5%) |
| T2 | 36 (13.8%) |
| T3 | 130 (50.0%) |
| T4 | 77 (29.6%) |
| Grade | |
| 1 | 97 (37.3%) |
| 2 | 109 (41.9%) |
| 3 | 37 (14.2%) |
| Unknown | 17 (6.5%) |
| Nodal (N) stage | |
| N0 | 220 (84.6%) |
| N1 | 17 (6.5%) |
| N2 | 23 (8.8%) |
| Alcohol abuse | |
| No | 66 (25.4%) |
| Mild | 81 (31.2%) |
| Moderate | 70 (26.9%) |
| Heavy | 43 (16.5%) |
| Smoking | |
| No | 13 (5.0%) |
| Ex | 20 (7.7%) |
| 1–20 p/y | 38 (14.6%) |
| 21–30 p/y | 35 (13.5%) |
| >30 p/y | 154 (59.2%) |
| Localization | |
| Glottic | 111 (42.7%) |
| Subglottic | 5 (1.9%) |
| Supraglottic | 123 (47.3%) |
| Transglottic | 21 (8.1%) |
| Type of surgery | |
| Total laryngectomy | 224 (86.2%) |
| Chordectomy | 15 (5.8%) |
| Other | 21 (8.1%) |
| Neck dissection | |
| No | 186 (71.5%) |
| Yes | 74 (28.5%) |
| Postoperative radiation | |
| No | 175 (67.3%) |
| Yes | 85 (32.7%) |
| Cohort II (N = 89) | |
| Age | |
| Median (range) | 63 (36–90) |
| Variable | No. of patients N = 89 |
| Gender | |
| Male | 84 (94.4%) |
| Female | 5 (5.6%) |
| Tumor stage | |
| T1 | 17 (19.1%) |
| T2 | 11 (12.4%) |
| T3 | 31 (34.8%) |
| T4 | 30 (33.7%) |
| Grade | |
| 1 | 12 (13.5%) |
| 2 | 36 (40.4%) |
| 3 | 41 (46.1%) |
| Nodes | |
| N0 | 69 (77.5%) |
| N1 | 15 (16.9%) |
| N2 | 5 (5.6%) |

(Continued on the following column)

Table 1. Clinicopathological features of the cohort I (N = 260) and cohort II (N = 89) of laryngeal SCC patients (Continued)

| Cohort II (N = 89) | |
|-------------------------|------------|
| Alcohol abuse | |
| No | 10 (11.2%) |
| Mild | 17 (19.1%) |
| Moderate | 32 (36.0%) |
| Heavy | 30 (33.7%) |
| Smoking | |
| No | 3 (3.4%) |
| Ex | 2 (2.2%) |
| 1–20 p/y | 1 (1.1%) |
| 21–30 p/y | 8 (9.0%) |
| >30 p/y | 74 (84.3%) |
| Localization | |
| Glottic | 51 (57.2%) |
| Subglottic | 2 (2.2%) |
| Supraglottic | 28 (31.5%) |
| Transglottic | 8 (9.0%) |
| Type of surgery | |
| Total laryngectomy | 52 (58.4%) |
| Chordectomy | 29 (32.6%) |
| Other | 8 (9.0%) |
| Neck dissection | |
| No | 70 (78.7%) |
| Yes | 19 (21.3%) |
| Postoperative radiation | |
| No | 39 (43.8%) |
| Yes | 50 (56.2%) |

flow chart of the study including the corresponding sample numbers is presented in Fig. 1A (REMARK diagram).

Quantitative IHC

For automated quantitative protein analysis, we used TMA sections, because the method operates more accurately on such histologic material (17). TMA sections were deparaffinized and stained as previously described using a non-commercial mouse monoclonal primary antibody to PD-L1 (clone 5H1, generated by Dr. Lieping Chen, Department of Immunobiology, Yale University, New Haven, CT) which had been validated in previous studies using quantitative IHC on neoplastic tissue and tumor cell lines (18, 19). For validation of PD-L1 antibody, a custom designed PD-L1 control TMA was used. This TMA contained samples from FFPE tissue blocks of human placenta and tonsil as positive controls for endogenous PD-L1, cores from FFPE prepared, parental Mel624 cells that do not express PD-L1 and Mel624 cells transfected with PD-L1 with proven overexpression, as well as a small series of NSCLC cases with previously measured high, low, and intermediate PD-L1 protein levels were also included. In brief, slides were deparaffinized with xylene and rehydrated through changes of ethanol with decreasing concentrations and they were then subjected to heat-induced antigen retrieval using tris-EDTA buffer (Sigma-Aldrich) with 0.05% Tween (pH.9.0) and boiling in a pressure-boiling container (PT module, Lab Vision) at 102°C for 20 minutes and then were incubated in 1% BlockAce (cat # BUF029, AbDSerotec) for 10 minutes at room temperature. Following these steps, slides were incubated with the previously described mouse monoclonal primary antiPD-L1 antibody at 1:500 dilution at 4°C overnight and an anti-cytokeratin antibody (rabbit anti-pancytokeratin antibody, 1:50, clone AE1/AE3, M3515, Dako Corporation) with subsequent goat anti-rabbit antibody conjugated to Alexa 546 fluorophore (1:100, A11035, Molecular Probes) in mouse

EnVision amplification reagent (K4003, Dako). We used DAPI to visualize nuclei (Prolong Gold with DAPI, P36931, Molecular Probes) and fluorescent chromogen Cy-5 tyramide (1:50, PerkinElmer Corp) for target identification.

Automated image acquisition and quantitative protein analysis

Automated image acquisition and analysis using automated *in situ* quantitative measurement of protein analysis (AQUA) has been described previously (17). In brief, monochromatic, high-resolution ($1,024 \times 1,024$ pixel; $0.5 \mu\text{m}$) images were obtained of each histospot. We distinguished areas of tumor from stromal elements by creating a mask from the cytokeratin signal. DAPI signal was used to identify nuclei, and the cytokeratin signal was used to define cytoplasm. Overlapping pixels (to a 99% confidence interval; CI) were excluded from both compartments. The signal (AQUA score) was scored on a normalized scale of 0 to 255 expressed as pixel intensity divided by the target area. AQUA scores for each subcellular compartment (nuclear and cytoplasmic) as well as the tumor mask were recorded. AQUA scores for duplicate tissue cores were averaged to obtain a mean score for each tumor. To verify antibody specificity, we used control TMA containing placenta and tonsil tissue (known to be positive for PD-L1) and pellets from MEL-624 cell lines, positive or negative for PD-L1 and NSCLC cases with previously measured levels of PD-L1 expression, as previously described (18, 20).

RNA extraction and PD-L1 expression quantification by qRT-PCR

A total of 145 tumor-containing paraffin blocks were available for RNA extraction and *PD-L1* expression quantification. RNA extraction from FFPE specimens was performed as previously described (9). Upon deparaffinization and overnight tissue fragment lysis with proteinase K at 56°C , RNA was extracted with TRIzol-LS Reagent (Life Technologies) and reverse transcribed with random primers and the Superscript III system (Life Technologies), according to the instructions of the manufacturer.

Total RNA from matched fresh-frozen tumor and normal adjacent tissue specimens of the cohort II of 89 laryngeal SCC patients was isolated by TRIzol Reagent (Life Technologies) and $2 \mu\text{g}$ of total RNA was reverse transcribed with oligo-dT primers and the MMLV reverse transcriptase (Life Technologies), according to the instructions of the manufacturer.

A SYBR Green-based qPCR assay was developed for the quantification of *PDL1* mRNA expression levels. Gene-specific primers were designed in order to span at least two exons, according to the mRNA sequences from the NCBI Sequence database, for *PDL1* (*CD274*) and *GAPDH* (NCBI RefSeq accession number: NM_014143.3 and NM_002046, respectively). More precisely, *PDL1* forward 5'-GTGGCATCCAAGATACAACTCAA-3' (exon 6) and reverse 5'-TCCTTCCTCTGTGACGCTCA-3' (exon 7) primers, and *GAPDH* forward 5'-ATGGGGAAGGTGAAGTTCG-3' (exon 2) and reverse 5'-GGTTCATTGATGGCAACAATATC-3' (exon 3) primers give rise to 147 bp and 107 bp specific products, respectively.

The amplification was performed in 96-well plates on an ABI Prism 7500 Real-Time PCR System (Applied Biosystems). The $10\text{-}\mu\text{L}$ reaction volume contained $5.0\text{-}\mu\text{L}$ of $2 \times$ KAPA SYBR FAST qPCR Master Mix (Kapa Biosystems), 200 nmol/L of each primer and 50 ng cDNA (either for FFPE samples or for tumor and normal adjacent tissue samples). The thermal protocol consisted of a

3-minute polymerase activation step at 95°C and 40 cycles of denaturation at 95°C for 15 seconds and primer annealing and extension at 60°C for 1 minute. Melting curve analysis was performed following amplification in order to distinguish the PCR products of interest from the nonspecific ones and primer dimers based on their different T_m .

Relative quantification of *PDL1* mRNA levels was performed by the $2^{-\Delta\Delta C_T}$ method, using the average C_T , as calculated from the duplicate reactions for each tested sample. *GAPDH* endogenous reference gene was used for normalization purposes and the CAL-33 cell line as our assay calibrator. Exclusion criteria for sample relative quantification analysis were *GAPDH* average C_T values higher than 33 for each duplicate.

Statistical analysis

For the analysis of PD-L1 expression levels between the different TILs groups of the patients according to Schalper and colleagues (21), the nonparametric Jonckheere–Terpstra test and Mann–Whitney *U* test were used, while the correlation of TILs percentage, PD-L1 protein and mRNA levels was performed by Spearman analysis. Wilcoxon signed rank test was used to evaluate the differences of PD-L1 mRNA levels between tumors and adjacent normal tissue specimens, while the nonparametric Jonckheere–Terpstra, Kruskal–Wallis, and Mann–Whitney *U* tests or the χ^2 test were performed for the analysis of TILs and PD-L1 expression levels, as continuous or categorical variables respectively, with the clinicopathological features of the patients.

The X-tile algorithm (22) was used for the adoption of optimal cut-off value of PD-L1 protein expression, which was equal to the 58th percentile of PD-L1 AQUA levels, whereas for PD-L1 mRNA levels, the median expression of the tumor samples was used as cut-off for each cohort. Kaplan–Meier survival curves using log-rank test and Cox proportional regression analysis were used in order to assess the prognostic significance of TILs, PD-L1 expression for the disease-free survival (DFS) and overall survival (OS) of the patients following treatment.

Results

Baseline clinical and experimental data

The cohort I of 260 tumors of primary laryngeal SCC was evaluated for stromal TILs as well as PD-L1 protein and mRNA levels. The clinicopathological characteristics of the patients are presented in Table 1. Management consisted of surgical resection of the tumor by means of total laryngectomy (86.2%) or by more conservative procedures (13.8%). A neck dissection was performed in 28.5% of cases, whereas postoperative external beam radiotherapy was administered in 32.7%.

Median patient age was 63.0 years. The majority of the patients were males (95.8%), current or ex-smokers (95.0%), and alcohol consumers (74.6%). As ex-smokers were characterized those individuals who discontinued tobacco at least 5 years before the diagnosis of larynx cancer. Ingestion of 15 to 18 g of alcohol two to three times a week was defined as mild alcohol consumption. As moderate and heavy alcohol use, we defined the daily uptake of 15 to 18 g and 30 or more g of alcohol, respectively. As shown in Table 1, diagnostic work-up led to diagnosis of laryngeal SCC predominantly supraglottic or glottic (90% of cases), mostly stage T3–4 (79.6% of cases) and more often node negative at clinical/radiologic examination (84.6%).

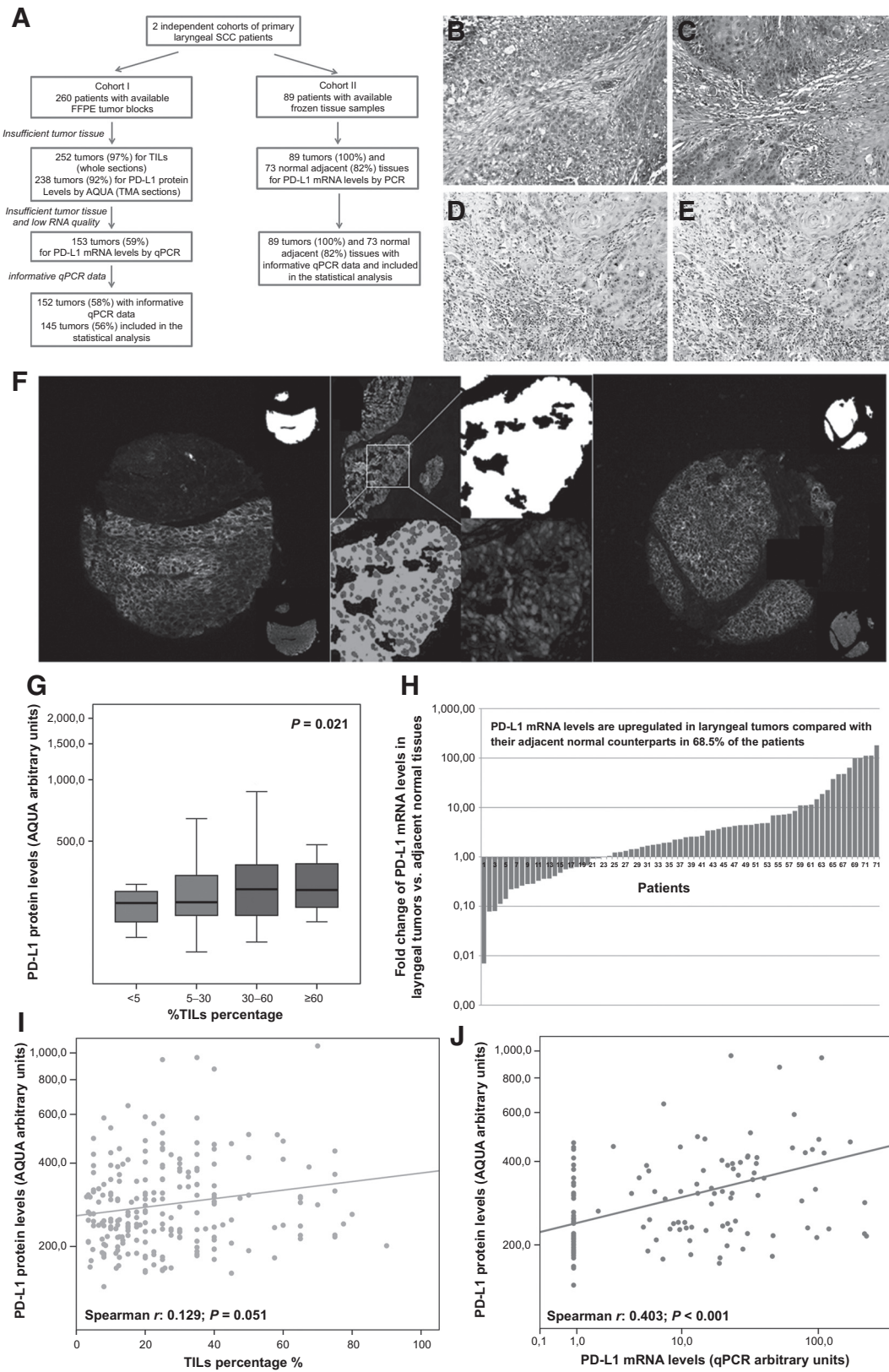


Figure 1. Evaluation of TILs and PD-L1 protein and mRNA levels in laryngeal SCC patients. A, REMARK diagram of patients' cohorts included in TILs and PD-L1 protein and mRNA analysis. (Continued on the following page.)

At a median follow-up time (reverse Kaplan–Meier method) of 75 months, 82 (31.5%) patients had relapsed and 107 (41.2%) had died. The median and 5-year DFS were 150 months (95% CI, 113.5–186.5 months) and 69.6%, respectively, whereas the median and 5-year OS were 106 months (95% CI, 87.8–124.2) and 65.4%, respectively. As expected, median OS was significantly shorter for patients with lymph node-positive disease as compared with those with lymph node-negative (28 vs. 107 months, $P = 0.001$) and for patients older than 63 years of age at diagnosis as compared with younger ones (87 vs. 142 months, $P = 0.008$). Compared with patients who had initially undergone more radical surgery (total laryngectomy), patients who had undergone more conservative surgery experienced statistically significant shorter median DFS (56 vs. 150 months, $P < 0.001$) but not OS (125 vs. 106 months, $P = 0.978$), probably due to the effect of salvage procedure.

Informative TILs and PD-L1 AQUA data were produced for 252 and 238 samples, respectively. On the basis of the criterion of tumor-cell content $>50\%$ and RNA quality, PD-L1 mRNA levels were measured in 153 FFPE specimens. Tumors excluded from this analysis did not differ from successfully evaluated tumors with respect to all parameters [age, $P = 0.382$; gender, $P = 0.356$; localization (glottis and subglottic vs. supraglottic), $P = 0.803$; grade, $P = 1.000$; T stage, $P = 0.106$; OS, $P = 0.761$; DFS, $P = 0.689$]. Using the exclusion criterion of *GAPDH* avg. C_T higher than 33 for each duplicate, 152 FFPE specimens yield informative qPCR data and 145 of them were included in the statistical analysis, as the remaining seven samples did not yield any data concerning TILs or PD-L1 protein levels (Fig. 1A). The final subset of tumors analyzed for *PD-L1* mRNA ($n = 145$) was equivalent to the whole population of 252 patients.

For cohort II, *PD-L1* mRNA levels were quantified in 89 tumors and 73 normal adjacent tissue specimens (Fig. 1A). The demographics and treatment characteristics of the second cohort are included in Table 1.

Higher TILs is strongly correlated with increased PD-L1 protein levels

According to TILs percentage, the patients ($N = 252$) were classified to low TILs cohort (161 patients; 63.8%) with $<30\%$ TILs, and the high TILs cohort (91 patients; 36.1%) having $\geq 30\%$ TILs according to Schalper and colleagues (21). Of the 161 patients of the low TILs group, 12 (4.8%) had $<5.0\%$ TILs and 149 (59.1%) had 5% to 30% TILs percentage. Similarly, the 91 patients of the high TILs group were further distinguished to 70 (27.8%) and 21 (8.3%) patients with 30% to 60% and $\geq 60\%$ TILs levels, respectively (Fig. 1B).

The percentage of stromal TILs was significantly associated with PD-L1 expression. Patients with high TILs percentage ($\geq 30\%$) were found to express higher PD-L1 protein levels ($P = 0.021$; Fig. 1C) compared with those with weaker infiltration ($<30\%$). A similar correlation was also observed for stromal TILs as a continuous variable. Spearman analysis supported a trend between

TILs density and tumor PD-L1 levels ($r_s = 0.129$; $P = 0.051$; Fig. 1D). PD-L1 mRNA levels were significantly correlated with PD-L1 protein levels ($r_s = 0.403$; $P < 0.001$; Fig. 1E), but not with TILs in Spearman analysis ($r_s = 0.130$; $P = 0.125$).

Analysis of TILs and PD-L1 expression with clinicopathological features

The analysis of PD-L1 mRNA levels in tumor specimens and normal adjacent tissues highlighted the overexpression of *PD-L1* gene in tumor cells. More precisely, laryngeal SCC tumors compared with their normal counterparts in 50 of the 73 evaluable patients (68.5%) expressed higher levels of *PD-L1* transcripts.

The analysis of TILs and PD-L1 expression with the clinicopathological features of the patients are presented in Supplementary Fig. S1 (continuous variable) and Supplementary Table S1 (categorical variable). Decreased TILs density was observed in patients with higher alcohol consumption ($P = 0.043$), whereas no statistically significant correlation was observed with T stage, grade, nodal stage, or smoking behavior. Concerning PD-L1, lower protein expression was noted in patients with higher smoking-index ($P = 0.022$), whereas stronger staining was observed in node-positive patients ($P = 0.018$). Finally, the study of PD-L1 mRNA levels in FFPE and fresh-frozen specimens did not reveal any statistically significant correlation with patients' and disease features.

TILs and PD-L1 protein expression represent independent predictors of laryngeal SCC patients' disease-free and overall survival

Kaplan–Meier and Cox proportional regression analysis performed for the evaluation of TILs and PD-L1 value to predict patients' DFS and OS following treatment.

The level of stromal TILs was strongly associated with superior survival outcome of the patients. Kaplan–Meier curves (Fig. 2A) highlighted the poor DFS ($P = 0.009$) of the patients with low TILs percentage compared with those with high TILs. Similarly, the patients with low stromal TILs demonstrated significantly worse OS ($P = 0.015$) compared with the high TILs group (Fig. 2B). The favorable outcome of the high TILs cohort was also supported by Cox regression analysis (Table 2). Univariate analysis (Table 2 and Fig. 2C and 2D) revealed the lower risk for disease relapse (HR, 0.542; 95% CI, 0.358–0.822; $P = 0.004$) and death (HR, 0.637; 95% CI, 0.462–0.880; $P = 0.006$) for the patients with high TILs.

The survival analysis also highlighted the favorable outcome of the patients overexpressing PD-L1 protein. Favorable DFS intervals and significantly lower risk for disease recurrence revealed by Kaplan–Meier curves ($P = 0.044$; Fig. 2E) and univariate Cox regression analysis (HR, 0.591; 95% CI, 0.351–0.996; $P = 0.048$; Table 2 and Fig. 2C) for the patients with higher PD-L1 expression compared with those with downregulated levels. Moreover, Kaplan–Meier analysis ($P = 0.059$; Fig. 2F) and univariate Cox regression (HR, 0.635; 95% CI, 0.393–1.024;

(Continued.) B–E, H&E sections (magnification $\times 100$) from four cases of operable laryngeal SCC evaluated for TILs as following: 3% (B), 20% (C), 50% (D), and 85% (E). F, AQUA image analysis for histospots positive for PD-L1. G, box plot representing the expression of PD-L1 protein levels related to TILs groups of laryngeal SCC patients, P value calculated by Jonckheere–Terpstra test. The middle lines inside the boxes indicate the median (50th percentile or second quartile). The lower and the upper box boundaries represent the 25th percentile (first quartile) and the 75th percentile (third quartile), respectively. The lower and upper whiskers extend to the lowest and highest value, respectively, within the $1.5\times$ interquartile range (box height) from the box boundaries. H, bar plot representing the fold change of PD-L1 mRNA levels in laryngeal SCC tumors compared with their normal adjacent tissues, P value calculated by Wilcoxon signed-rank test. I and J, Spearman correlation analysis of PD-L1 protein levels with (I) TILs, and (J) PD-L1 mRNA levels. r , Spearman correlation coefficient.

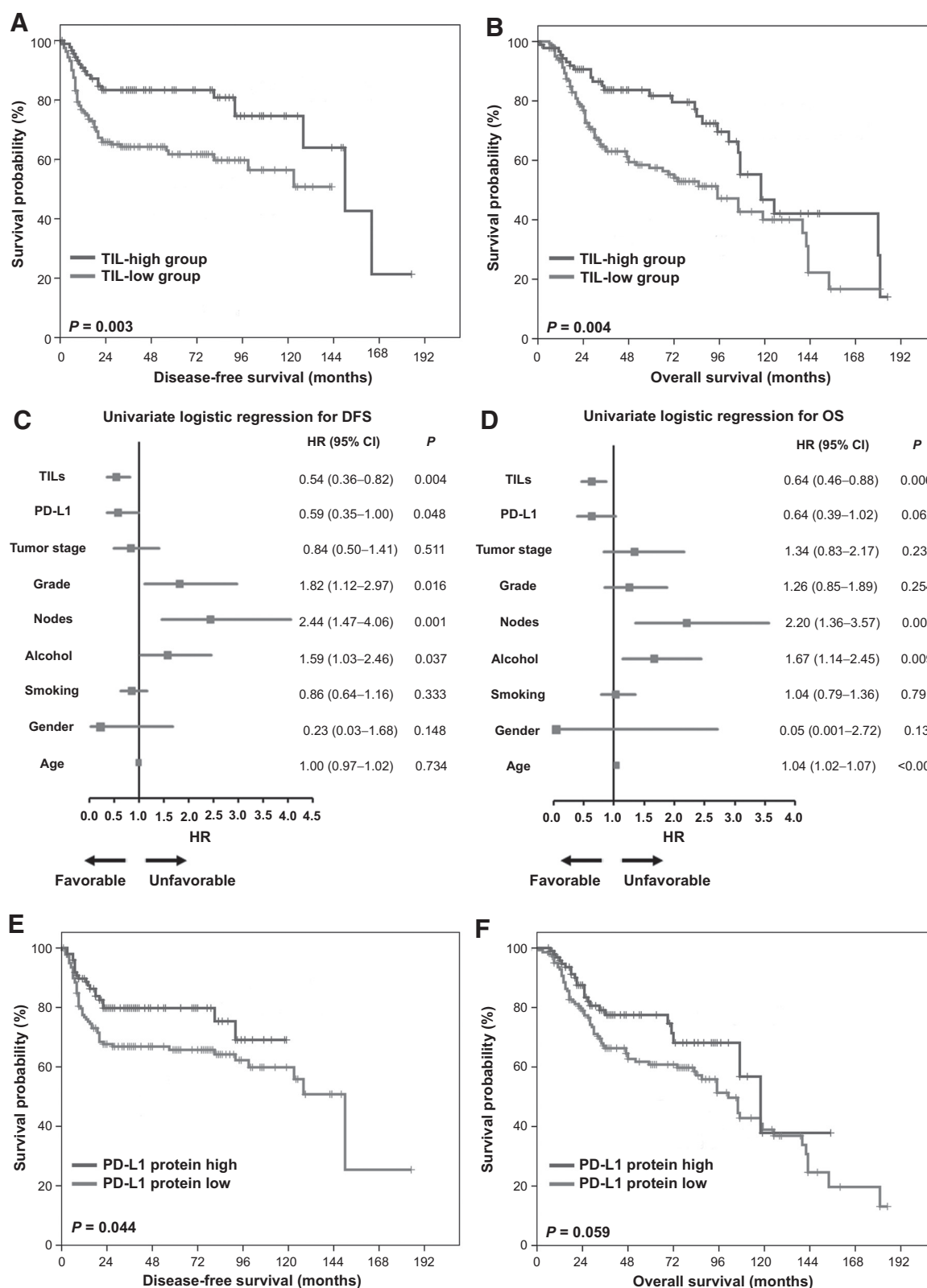


Figure 2. PD-L1 and TILs density correlate with superior DFS and OS of the laryngeal SCC patients. A and B, Kaplan-Meier curves for the analysis of laryngeal SCC patients (A) DFS and (B) OS according to TILs density, P values calculated by log-rank test. C and D, Forrest plot of the univariate Cox regression analysis for the prediction of laryngeal SCC patients (C) DFS and (D) OS. E and F, Kaplan-Meier curves for the analysis of laryngeal SCC patients (E) DFS and (F) OS according to PD-L1 protein levels, P values calculated by log-rank test.

Table 2. Cox proportional regression analysis for the prediction of laryngeal SCC patients' DFS and OS following treatment

| Covariant | DFS | | | |
|---|--|----------------|--|----------------|
| | Univariate analysis | | Multivariate analysis | |
| | HR ^a (95% CI ^b) | P ^c | HR ^a (95% CI ^b) | P ^c |
| TILs (<30 vs. 30–60 vs. ≥60%) | 0.542 (0.358–0.822) | 0.004 | 0.587 (0.381–0.903) | 0.015 |
| PD-L1 protein levels (overexpression ^d) | 0.591 (0.351–0.996) | 0.048 | 0.532 (0.301–0.941) | 0.030 |
| Tumor stage (T1/T2 vs. T3/T4) | 0.841 (0.502–1.409) | 0.511 | 0.575 (0.323–1.024) | 0.060 |
| Grade (1 vs. 2/3) | 1.823 (1.120–2.968) | 0.016 | 1.247 (0.709–2.196) | 0.444 |
| Nodes (N0 vs. N+) | 2.439 (1.465–4.061) | 0.001 | 3.635 (1.852–7.133) | <0.001 |
| Alcohol consumption (no/mild vs. moderate/high) | 1.588 (1.027–2.455) | 0.037 | 2.118 (1.268–3.538) | 0.004 |
| Smoking behavior (no/ex vs. moderate vs. heavy) | 0.862 (0.638–1.164) | 0.333 | 0.762 (0.533–1.089) | 0.136 |
| Gender (male vs. female) | 0.234 (0.032–1.679) | 0.148 | <0.001 | 0.972 |
| Age | 0.996 (0.972–1.020) | 0.734 | 0.989 (0.961–1.018) | 0.452 |

| Covariant | OS | | | |
|---|--|----------------|--|----------------|
| | Univariate analysis | | Multivariate Analysis | |
| | HR ^a (95% CI ^b) | P ^c | HR ^a (95% CI ^b) | P ^c |
| TILs (<30 vs. 30–60 vs. ≥60%) | 0.637 (0.462–0.880) | 0.006 | 0.609 (0.430–0.862) | 0.005 |
| PD-L1 protein levels (overexpression ^d) | 0.635 (0.393–1.024) | 0.062 | 0.570 (0.333–0.973) | 0.039 |
| Tumor stage (T1/T2 vs. T3/T4) | 1.341 (0.828–2.169) | 0.233 | 0.904 (0.526–1.553) | 0.715 |
| Grade (1 vs. 2/3) | 1.263 (0.845–1.887) | 0.254 | 0.931 (0.584–1.485) | 0.765 |
| Nodes (N0 vs. N+) | 2.200 (1.357–3.565) | 0.001 | 4.516 (2.347–8.689) | <0.001 |
| Alcohol consumption (no/mild vs. moderate/high) | 1.671 (1.140–2.449) | 0.009 | 1.816 (1.165–2.828) | 0.008 |
| Smoking behavior (no/ex vs. moderate vs. heavy) | 1.037 (0.792–1.359) | 0.791 | 0.924 (0.674–1.265) | 0.621 |
| Gender (male vs. female) | 0.046 (0.001–2.722) | 0.139 | <0.001 | 0.970 |
| Age | 1.044 (1.020–1.069) | <0.001 | 1.046 (1.018–1.075) | 0.001 |

^aHazard ratio.

^bConfidence interval of the estimated HR.

^cTest for trend.

^dCut-off value was equal to the 59th percentile of PD-L1 AQUA score.

P = 0.062; Table 2 and Fig. 2D) highlighted the trend of the patients overexpressing PD-L1 for superior OS outcome.

Multivariate Cox regression models, adjusted for tumor stage, grade, nodal status, alcohol consumption, smoking behavior, age, and gender, were used for the evaluation of the independent prognostic value of TILs and PD-L1 (Table 2). Both high stromal TILs (HR, 0.587; 95% CI, 0.381–0.903; *P* = 0.015) and PD-L1 protein levels (HR, 0.532; 95% CI, 0.301–0.941; *P* = 0.030) were independent predictors of patients' superior DFS. Similarly, multivariate Cox models proved the independent correlation of higher stromal TILs (HR, 0.604; 95% CI, 0.430–0.862; *P* = 0.005) and PD-L1 protein levels (HR, 0.570; 95% CI, 0.333–0.973; *P* = 0.039) with the longer OS interval of the patients following treatment.

In addition, we studied the clinical value of PD-L1 mRNA levels for laryngeal SCC prognosis. For this survival analysis, the median PD-L1 expression of the tumor samples was used as cut-off for each cohort. Focusing on the first patients' cohort, Kaplan–Meier survival curves (Supplementary Fig. S2) and Cox regression analysis (Supplementary Table S2) did not highlight any significant correlation between PD-L1 mRNA level in FFPE specimens (*N* = 145) and patients risk for relapse or death. This was also noted in the survival analysis of the second independent cohort of laryngeal SCC patients. More precisely, the analysis of PD-L1 mRNA levels in fresh-frozen tumor specimens (*N* = 89), did not reveal any significance for the prognosis of patients (Supplementary Fig. S2 and Supplementary Table S2).

Discussion

Recent studies indicate that evaluation of PD-L1 status in tumor specimens could assist in patient selection for treatment

with PD1 checkpoint inhibitors. However, accurate measurement of PD-L1 protein levels in FFPE tumor samples is limited by the absence of reliable antibodies and interpretative uncertainties (i.e., positivity cutoff). With the recent unprecedented success of PD-1/PD-L1 targeting antibodies for treating several cancers, our purpose was to characterize PD-L1 and TIL expression in primary laryngeal cancers. We describe here evaluation of PD-L1 protein by a more quantitative method of PD-L1 determination which avoids bias introduced by the subjectivity of pathologist-based scoring. We also used a validated antibody generated by Dr. Lieping Chen. High TIL content was a strong favorable prognostic indicator for both DFS and OS and retained significance in multivariate analysis. High PD-L1 expression was associated with improved DFS and OS on both uni- and multivariate analysis. Our results are not in agreement with previous studies demonstrating an adverse prognostic effect of PD-L1 expression by IHC in several cancers including renal, colorectal, and lung cancers (23–25). Other studies in metastatic melanomas, non-small cell lung cancer, Merkel cell carcinomas, by using the validated antibody clone 5H1, they demonstrated a positive association of high PD-L1 expression and elevated TILs with longer survival (26–28).

We also found a significant positive association between PD-L1 expression and TIL level. The biologic determinants of the association between PD-L1 expression, increased TILs, and improved outcome are not well understood. For instance, in T-cell inflamed melanomas infiltration by CD8-positive T lymphocytes was associated with high expression of immunosuppressive elements such as T_{regs}, PD-L1 protein and mRNA, and IDO expression. Furthermore, induction of these immune inhibitory pathways in the tumor microenvironment depended on the presence of CD8-positive T cells and IFN in a murine model (29). Therefore, it is possible that rather than an

indication of total immune escape, PD-L1 expression by tumor cells might reflect the presence of antigen-induced antitumor immune pressure mediated by TILs. Although only partially effective, recruitment of TILs to the tumor microenvironment in response to preserved chemotactic signals could still induce a partial antitumor effect and explain the observed survival benefit. PD-L1 expression is upregulated by T-cell secretion of IFN γ and patients with T-cell rich tumors expressing PD-L1 are likely to have better immune surveillance (26). It is therefore possible that PD-L1 and TIL levels can select patients for treatment with immune checkpoint inhibitors.

Published predictive correlative studies done on multi-institutional trials have mainly focused on PD-L1 expression. Although this clearly is associated with TIL content, our findings, along with the findings of other investigators (18), suggest that TILs could be included in predictive biomarker studies of patients treated with checkpoint inhibitors. This has been done in a small single institution study of multiple tumor types (renal cell carcinoma, lung cancer, melanoma) treated with nivolumab (20). In this study, tumor PD-L1 expression remained the strongest predictor for response to nivolumab, but it is possible that a model combining both TIL and PD-L1 might best predict response to checkpoint inhibitors. Studies evaluating the prognostic value of T-cell subsets in melanoma have demonstrated that the percent of CD8-positive cells are independent predictors for improved survival (18). It is therefore possible that T-cell subsets have differential effect on prognosis and prediction for response to PD-1/PD-L1 checkpoint inhibitors. Balermias and colleagues (30) also reported that robust tumor infiltration by CD3⁺ and CD8⁺ cytotoxic T cells are associated with improved prognosis upon definitive chemoradiotherapy in HNSCC. The prognostic importance of tumor infiltration with CD3⁺ and CD8⁺ cells has been demonstrated in breast, esophageal, lung, ovarian, colon, and anal cancers (31). In addition, Balermias and colleagues (30) reported that the intratumoral localization of TILs (in close proximity of tumor cells, in the tumor stroma and in the periphery) influences their prognostic impact. Recent studies by Taube and colleagues (20) and Tumei and colleagues (32) have also demonstrated that the location of T-cell infiltrate and PD-L1-expressing cells within a tumor specimen is of particular importance; detection of CD8⁺ TILs and PD-L1-expressing cells at the invasive margin was associated with better response to therapy. In our study, TILs were present in almost all cases in tumor invasive front.

Studies evaluating the association of PD-L1 expression and response to PD-1/PD-L1 checkpoint inhibitors, despite the utilization of variable cutpoints and reagents, consistently demonstrate that patients whose tumors express PD-L1 are more likely to respond to therapy. We used a more quantitative method of PD-L1 determination that avoids bias introduced by the subjectivity of pathologist-based scoring. The strong association between PD-L1 expression and TILs further supports the findings of Tumei and colleagues (32), who found close proximity between PD-1 and PD-L1-expressing cells.

In our study, we did not find a correlation between *PD-L1* mRNA expression and outcome in two independent cohorts of HNSCC although a strong association between *PD-L1* mRNA and PD-L1 protein levels was noted. The difference might be explained, at least in part, by the distinct properties and independent information provided by PD-L1 protein and mRNA

molecules, as reported (33). Methodologic differences might also account for the apparent inconsistency.

Our analysis has a number of limitations. One limitation is that it includes retrospectively collected cases. A second limitation is that the use of TMAs may underestimate or overestimate the PD-L1 protein levels due to intratumoral heterogeneity of expression. Although our results support the value of measuring PD-L1 protein in TMA samples, translation of these findings into the clinical setting could certainly benefit from using whole tissue section samples. Determination of the amount of tumor tissue that is required for accurate assessment of PD-L1 expression should be further evaluated but should likely consider tumor size, availability of tissue material (core vs. tumor resection), clinical objective (prognostic vs. predictive), and disease setting (one primary vs. multiple primaries vs. disseminated disease). Another limitation of our method is the inability to distinguish within the tumor mask PD-L1 T cell expression from PD-L1 cancer cell expression or PD-L1 expression on macrophages. Herbst and colleagues (34) demonstrated that PD-L1 expression on TILs predicted for response to MPDL2380A anti-PD-L1 antibody across multiple tumor types. Newer *in situ* multiplex methods are being developed which might facilitate assessment of PD-L1 expression in different cell types, such as macrophages, within the tumor microenvironment.

In summary, our study demonstrates, for the first time, the association between PD-L1 protein expression using automated quantitative analysis and improved prognosis in HNSCC. We also show the association between PD-L1 expression and TILs in HNSCC. Furthermore, TIL level was an independent predictor for improved outcome and retained independence on multivariate analysis. Biomarker studies of patients treated with PD-1/PD-L1 inhibitors will determine the predictive value of PD-L1 AQUA levels and TILs for response to these therapies.

Disclosure of Potential Conflicts of Interest

V. Velcheti is a consultant/advisory board member for Clovis, Foundation Medicine, and Novartis. D. Rimm reports receiving commercial research grants from Cepheid, Genoptix, and Gilead Sciences; holds ownership interest (including patents) in Metamark Genetics, and is a consultant/advisory board member for Biocept, Bristol-Myers Squibb, Cernostics, MDAGree, Metamark Genetics, and Perkin Elmer. No potential conflicts of interest were disclosed by the other authors.

Authors' Contributions

Conception and design: M. Avgeris, C. Perisanidis, A. Psyrri
Development of methodology: M. Avgeris, V. Velcheti, G. Fountzilias
Acquisition of data (provided animals, acquired and managed patients, provided facilities, etc.): M. Vassilakopoulou, M. Avgeris, V. Velcheti, V. Kotoula, T. Rampias, K. Chatzopoulos, A.I. Giotakis, D. Rimm, G. Fountzilias, A. Psyrri
Analysis and interpretation of data (e.g., statistical analysis, biostatistics, computational analysis): M. Vassilakopoulou, M. Avgeris, V. Velcheti, T. Rampias, K. Chatzopoulos, C. Perisanidis, A. Scorilas, A. Psyrri
Writing, review, and/or revision of the manuscript: M. Vassilakopoulou, M. Avgeris, V. Velcheti, V. Kotoula, K. Chatzopoulos, A.I. Giotakis, C. Sasaki, G. Fountzilias, A. Psyrri
Administrative, technical, or material support (i.e., reporting or organizing data, constructing databases): M. Vassilakopoulou, V. Velcheti, C. Perisanidis, C.K. Kontos, A.I. Giotakis, A. Scorilas, A. Psyrri
Study supervision: C. Perisanidis, C.T. Sasaki, A. Psyrri
Other (organized patient data and carried out part of the experimental work): C.K. Kontos

Received June 29, 2015; revised September 2, 2015; accepted September 2, 2015; published OnlineFirst September 25, 2015.

References

1. Lyford-Pike S, Peng S, Young GD, Taube JM, Westra WH, Akpeng B, et al. Evidence for a role of the PD-1:PD-L1 pathway in immune resistance of HPV-associated head and neck squamous cell carcinoma. *Cancer Res* 2013;73:1733–41.
2. Badoual C, Hans S, Merillon N, Van Ryswick C, Ravel P, Benhamouda N, et al. PD-1-expressing tumor-infiltrating T cells are a favorable prognostic biomarker in HPV-associated head and neck cancer. *Cancer Res* 2013;73:128–38.
3. Fury M, Ou SI, Balmanoukian A, Hansen A, Massarelli E, Blake-Haskins A, et al. Clinical activity and safety of MEDI4736, an anti-PD-L1 antibody, in patients with head and neck cancer. *Ann Oncol* 2014;25:iv341.
4. Chow LQ, Burtneis B, Weiss J, Berger R, Eder JP, Gonzalez EJ, et al. A phase Ib study of pembrolizumab (pembro; MK-3475) in patients (pts) with human papilloma virus (HPV)-positive and negative head and neck cancer (HNC). *Ann Oncol* 2014;25:v1–v41.
5. Brahmer JR. Harnessing the immune system for the treatment of non-small-cell lung cancer. *J Clin Oncol* 2013;31:1021–8.
6. Hamid O, Schmidt H, Nissan A, Ridolfi L, Aamdal S, Hansson J, et al. A prospective phase II trial exploring the association between tumor micro-environment biomarkers and clinical activity of ipilimumab in advanced melanoma. *J Transl Med* 2011;9:204.
7. Sznol M, Chen L. Antagonist antibodies to PD-1 and B7-H1 (PD-L1) in the treatment of advanced human cancer. *Clin Cancer Res* 2013;19:1021–34.
8. Pardoll DM. The blockade of immune checkpoints in cancer immunotherapy. *Nat Rev Cancer* 2012;12:252–64.
9. Fountzilias E, Kotoula V, Angouridakis N, Karasmanis I, Wirtz RM, Eleftheraki AG, et al. Identification and validation of a multigene predictor of recurrence in primary laryngeal cancer. *PLoS ONE* 2013;8:e70429.
10. McShane LM, Altman DG, Sauerbrei W, Taube SE, Gion M, Clark GM. Reporting recommendations for tumour MARKer prognostic studies (REMARK). *Br J Cancer* 2005;93:387–91.
11. Loi S, Sirtaine N, Piette F, Salgado R, Viale G, Van Eenoo F, et al. Prognostic and predictive value of tumor-infiltrating lymphocytes in a phase III randomized adjuvant breast cancer trial in node-positive breast cancer comparing the addition of docetaxel to doxorubicin with doxorubicin-based chemotherapy: BIG 02–98. *J Clin Oncol* 2013;31:860–7.
12. Loi S, Michiels S, Salgado R, Sirtaine N, Jose V, Fumagalli D, et al. Tumor infiltrating lymphocytes are prognostic in triple negative breast cancer and predictive for trastuzumab benefit in early breast cancer: results from the FinHER trial. *Ann Oncol* 2014;25:1544–50.
13. Salgado R, Denkert C, Demaria S, Sirtaine N, Klauschen F, Pruneri G, et al. The evaluation of tumor-infiltrating lymphocytes (TILs) in breast cancer: recommendations by an International TILs Working Group 2014. *Ann Oncol* 2015;26:259–71.
14. West NR, Milne K, Truong PT, Macpherson N, Nelson BH, Watson PH. Tumor-infiltrating lymphocytes predict response to anthracycline-based chemotherapy in estrogen receptor-negative breast cancer. *Breast Cancer Res* 2011;13:R126.
15. Rathore AS, Kumar S, Konwar R, Makker A, Negi MP, Goel MM. CD3⁺, CD4⁺ and CD8⁺ tumour infiltrating lymphocytes (TILs) are predictors of favourable survival outcome in infiltrating ductal carcinoma of breast. *Indian J Med Res* 2014;140:361–9.
16. Galon J, Mlecnik B, Bindea G, Angell HK, Berger A, Lagorce C, et al. Towards the introduction of the 'Immunoscore' in the classification of malignant tumours. *J Pathol* 2014;232:199–209.
17. Camp RL, Chung GG, Rimm DL. Automated subcellular localization and quantification of protein expression in tissue microarrays. *Nat Med* 2002;8:1323–7.
18. Kluger HM, Zito CR, Barr ML, Baine MK, Chiang VL, Sznol M, et al. Characterization of PD-L1 Expression and Associated T-cell Infiltrates in Metastatic Melanoma Samples from Variable Anatomic Sites. *Clin Cancer Res* 2015;21:3052–60.
19. Velcheti V, Schalper KA, Carvajal DE, Anagnostou VK, Syrigos KN, Sznol M, et al. Programmed death ligand-1 expression in non-small cell lung cancer. *Lab Invest* 2014;94:107–16.
20. Taube JM, Klein A, Brahmer JR, Xu H, Pan X, Kim JH, et al. Association of PD-1, PD-1 ligands, and other features of the tumor immune microenvironment with response to anti-PD-1 therapy. *Clin Cancer Res* 2014;20:5064–74.
21. Schalper KA, Velcheti V, Carvajal D, Wimberly H, Brown J, Pusztai L, et al. In situ tumor PD-L1 mRNA expression is associated with increased TILs and better outcome in breast carcinomas. *Clin Cancer Res* 2014;20:2773–82.
22. Camp RL, Dolled-Filhart M, Rimm DL. X-tile: a new bio-informatics tool for biomarker assessment and outcome-based cut-point optimization. *Clin Cancer Res* 2004;10:7252–9.
23. Mu CY, Huang JA, Chen Y, Chen C, Zhang XG. High expression of PD-L1 in lung cancer may contribute to poor prognosis and tumor cells immune escape through suppressing tumor infiltrating dendritic cells maturation. *Med Oncol* 2011;28:682–8.
24. Song M, Chen D, Lu B, Wang C, Zhang J, Huang L, et al. PTEN loss increases PD-L1 protein expression and affects the correlation between PD-L1 expression and clinical parameters in colorectal cancer. *PLoS ONE* 2013;8:e65821.
25. Konishi J, Yamazaki K, Azuma M, Kinoshita I, Dosaka-Akita H, Nishimura M. B7-H1 expression on non-small cell lung cancer cells and its relationship with tumor-infiltrating lymphocytes and their PD-1 expression. *Clin Cancer Res* 2004;10:5094–100.
26. Taube JM, Anders RA, Young GD, Xu H, Sharma R, McMiller TL, et al. Colocalization of inflammatory response with B7-1 expression in human melanocytic lesions supports an adaptive resistance mechanism of immune escape. *Sci Transl Med* 2012;4:127ra37.
27. Lipson EJ, Vincent JC, Loyo M, Kagohara LT, Lubner BS, Wang H, et al. PD-L1 expression in the Merkel cell carcinoma microenvironment: association with inflammation, Merkel cell polyomavirus and overall survival. *Cancer Immunol Res* 2013;1:54–63.
28. Droezer RA, Hirt C, Viehl CT, Frey DM, Nebiker C, Huber X, et al. Clinical impact of programmed cell death ligand 1 expression in colorectal cancer. *Eur J Cancer* 2013;49:2233–42.
29. Spranger S, Spaepen RM, Zha Y, Williams J, Meng Y, Ha TT, et al. Up-regulation of PD-L1, IDO, and T(regs) in the melanoma tumor microenvironment is driven by CD8(+) T cells. *Sci Transl Med* 2013;5:200ra116.
30. Balermipas P, Rodel F, Liberz R, Oppermann J, Wagenblast J, Ghanaati S, et al. Head and neck cancer relapse after chemoradiotherapy correlates with CD163⁺ macrophages in primary tumour and CD11b⁺ myeloid cells in recurrences. *Br J Cancer* 2014;111:1509–18.
31. Gooden MJ, de Bock GH, Leffers N, Daemen T, Nijman HW. The prognostic influence of tumour-infiltrating lymphocytes in cancer: a systematic review with meta-analysis. *Br J Cancer* 2011;105:93–103.
32. Tumeh PC, Harview CL, Yearley JH, Shintaku IP, Taylor EJ, Robert L, et al. PD-1 blockade induces responses by inhibiting adaptive immune resistance. *Nature* 2014;515:568–71.
33. Bordeaux JM, Cheng H, Welsh AW, Haffty BC, Lannin DR, Wu X, et al. Quantitative in situ measurement of estrogen receptor mRNA predicts response to tamoxifen. *PLoS ONE* 2012;7:e36559.
34. Herbst RS, Soria JC, Kowanetz M, Fine GD, Hamid O, Gordon MS, et al. Predictive correlates of response to the anti-PD-L1 antibody MPDL3280A in cancer patients. *Nature* 2014;515:563–7.